Journal of Ovonic Research Vol. 17, No. 6, November – December 2021, p. 581 - 587

Structural and optical characterization of nanostructured undoped CuO and cobalt - doped CuO thin films

Zaid A. Abed*, Ali H. Al Dulaimi, Wafaa A. Shatti, Ahmed N. Jasim,
Ziad T. Khodair, Sura Y. Khaleel
University of Diyala, College of Science, Physics Department, Iraq

The undoped CuO and CuO:Co films are grown using spray pyrolysis technique(SPT). The deposited films undergo a clear morphological change due to an increase in Cobalt dopant from 0 to 4 %. The predominant peak was (200) plane has been confirmed by X-ray diffraction. Maximum crystalline size was at the (CuO: 4% Co) film, and the strain decreases from 2.98 to 2.59. Study of the morphology specifies the presence of homogeneous grains, these grains were not homogeneous and had different sizes by adding Co atom. AFM images a reduction in roughness from (7.06 to 3.64) nm. The crystallite size was in the area of 41.35 nm to 32.46 nm as calculated by Scherrer's formula. The average transmittance values for the films were (77, 74 and 71) % for Undoped CuO, CuO: 2% Co and CuO: 4% Co respectively. The optical energy gaps of the films were calculated. the absorption coefficient increased with an increase at 2% or 4% Cobalt dopant, the band gap of Undoped CuO sample was 2.12 eV, and then decreased slightly with Cobalt content to become 2.04 eV for CuO: 2% Co and 2.04 eV for CuO: 4% Co. also The refractive index and extinction coefficient increased via Cobalt contents.

(Received September 17, 2021; Accepted December 15, 2021)

Keywords: Pure CuO thin film, Cobalt content, Structural properties, Optical properties, Energy gap

1. Introduction

CuO is a semiconducting material that fabricated and characterized, and then involved by diverse interesting applications [1, 2]. CuO and Cu2O are employed as p-n junction diodes [3], electrode materials for lithium batteries [4, 5]. CuO thin film is utilized as field effect transistors and gas sensors [6], solar cells [7] and electronics [8-10]. It has direct optical band gap energy ranging from 2.1 to 2.6 eV [11]. CuO can be synthesis using different methods including sputtering [12, 13], thermal evaporation and oxidation [14], MBE [15], electrochemical deposition [16]. chemical vapor deposition [17] electro-deposition [18], sol gel techniques [19PLD [20] and SPT [21]. In this study, CuO thin films were grown by SPT, which can produce large- area films with respectable properties. These films were characterized by XRD, AFM and ultraviolet–visible (UV–vis) spectroscopy, the experiments were carried out to study the effect of adding Cobalt as a dopant.

2. Experimental part

Thin films of undoped CuO and CuO: Co films have been deposited by SPT. A lab-designed glass atomizer with output nozzle of 1 mm has been used to spray 0.1 M solution of Cu [C4H6CuO4] on glass substrates at a temperature of 350°C. The doping employed was (CoCl3) resolve by redistilled water, and drops of HCl were joined the solution to get it clear. Optimum deposition parameters given in Table 1.

* Corresponding author: alialdulimi1985@gmail.com

Table 1. Optimum deposition parameter of spray solutions.

Deposition Parameters	Value
spray time	8 sec
spray period	2 min
Carrier gas	air at a pressure of 10^5 Nm^{-2}
distance between spout and base	30 cm ±1 cm
solution flow rate	5 ml/min

The samples were weighted before and after spraying to obtain film mass. Thickness of the fabricated films was measured to be around 320 nm. Absorption and transmission spectra were examined by double beam UV/VIS. Structural properties were evaluated by XRD, AFM was utilized to obtain film surface

3. Results and Discussion

XRD was implemented to certain the crystal structure and orientation of prepared films. The XRD spectra of undoped CuO and CuO: Co recorded in 2θ angle ranging from 20º to 70 º are depicted in Fig. 1. These results indicate the grown films were polycrystalline peaks appeared at (110), (200), (202) and (022) planes, which is fitted with ICDD card no. (041-0254). Strong peak was appearing toward (200). It can be easily noted that the intensity peaks increase with Cobalt doping conforming an improvement in the films crystallinity.

Mean crystallite size was calculated for the [200] diffraction peak using Scherrer formula:[23].

$$D = \frac{0.9\lambda}{\beta cos\theta}$$

where λ is X-rays wavelength, β is (FWHM).

Table 2 shows that the crystallite sizes are (11.73 nm), (12.37) and (13.34) for Undoped CuO and CuO: 2% Co and CuO: 4% Co thin films respectively, The increment in cobalt doping results in grain growth thereby an increase in crystallite size,

The dislocation density (δ) in thin films were obtained via the relation [24]:

$$\delta = \frac{1}{D^2}$$

the dislocation density (δ) parameter decreases from 7.26 to 5.61,

The strain (ε) is evaluated by utlizingthe following equation [25]:

$$\varepsilon = \frac{\beta cos\theta}{4}$$

It can be noted that ε values decrease with cobalt content, the obtained structural parameters Spara are displayed in Table 1. Figure (2) offers FWHM, D, δ and ε versus Cobalt dopant.

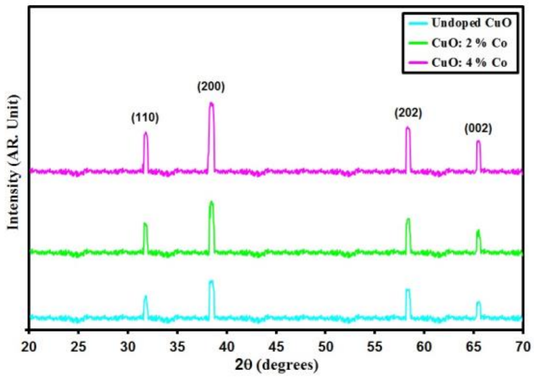

Fig.1. XRD patterns of the prepared films.

Table 2. D, band gap and Spara of the grown films.

Samples	2 θ (°)	(hkl) Plane	FWHM (°)	E_g(eV)	D (nm)	Dislocations density (× 10^{15})(lines/m^2)	Strain (× 10^{-3})
Undoped CuO	38.65	200	0.72	2.12	11.73	7.026	2.98
CuO: 2% Co	38.30	200	0.68	2.08	12.37	6.55	2.80
CuO:4% Co	38.00	200	0.63	2.04	13.34	5.61	2.59

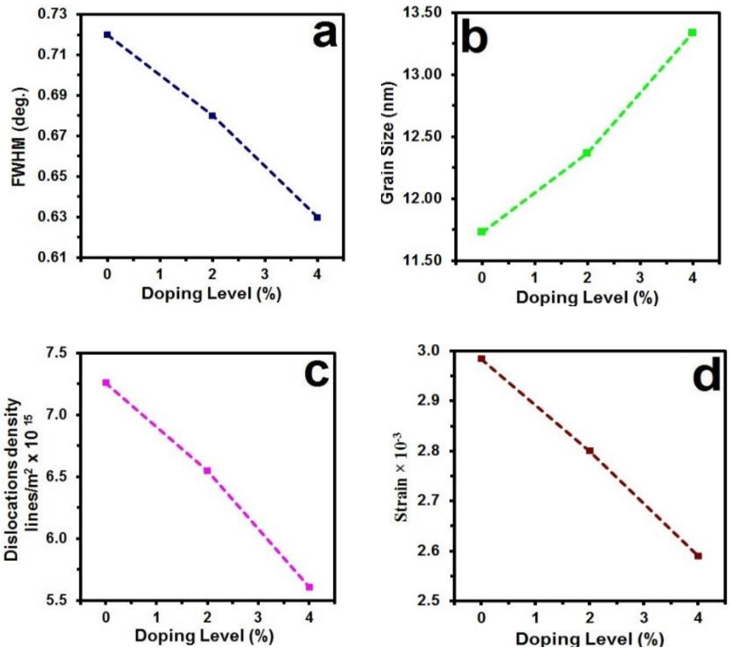

Fig. 2. FWHM (a) D (b) δ (c) ε (d) versus doping.

Fig. 3. Shows AFM images of the grown films. The root mean square (Rrms) or average roughness Ra is displayed in Table 3. These images show that films are dole out uniformly in shape of small granules without spaces between them. Figure 3 (a2, b2 and c2) offers a volumetric distribution of crystalline granules [38, 39], From Fig. 3 (a3, b3 and c3). The mean particle size was measured to be 41.35 nm to 32.46 nm, (Ra) and (Rrms) values are (7.05, 5.08 and 3.64) nm and (5.82, 4.53 and 2.27) nm, for CuO and CuO: Co respectively. The above results mention that

Ra and Rrms are influenced via Cobalt Content Table (3) represent the values of AFM parameters PAFM.

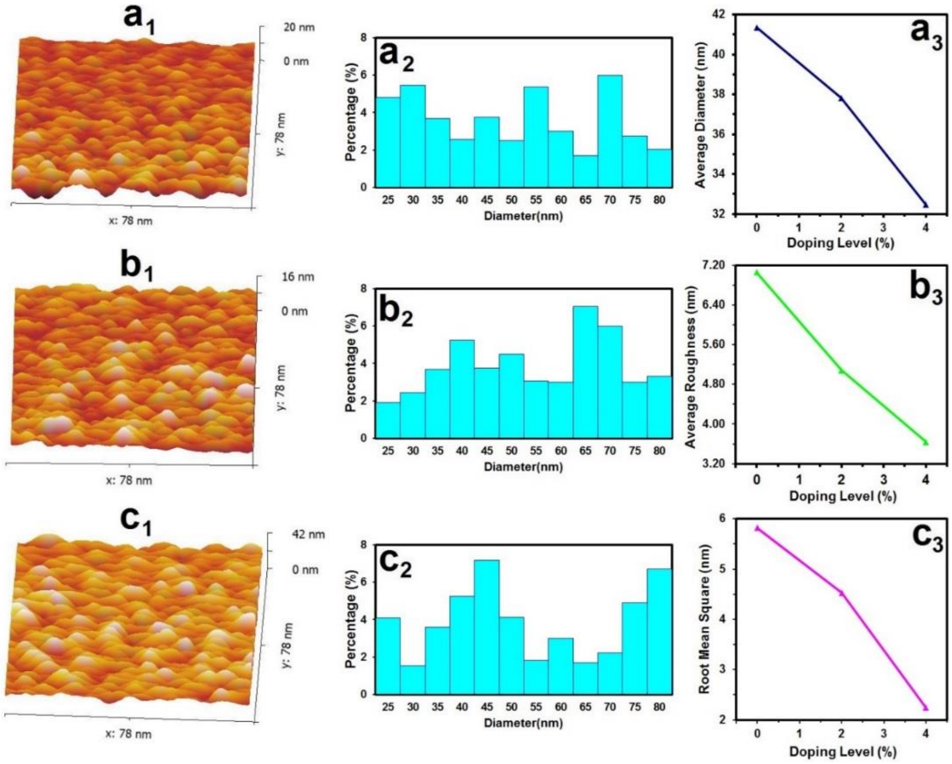

Fig. 3. AFM images (a1, b1 and c1), granularly distributed (a2, b2 and c2) and variation of PAFM via doping (a3, b3 and c3).

Table 3. PAFM of the grown films.

Samples	Average Particle size nm	R_a (nm)	R_{rms}. (nm)
Undoped CuO	41.35	7.06	5.82
CuO: 2% Co	37.82	5.08	4.53
CuO:4% Co	32.46	3.64	2.27

Optical properties of Undoped CuO and doped with Cobalt with concentration 2% and 4% samples recorded in the wavelength range 300-900nm and drawn in fig. 3 represent the variation of transmittance against wavelength and indicate the same behavior of high transparency in the visible and near infrared window. These spectra were decreasing with Cobalt doping of all wavelength ranges. The transmittance ranges from 76 to 70 % at the wavelength around (600 - 900) nm, it was noticed that transmittance T decrease with Cobalt content. The absorption coefficient (α) of the films calculated this relation [26]:

$$\alpha = (2.303\times A)/t \qquad (4)$$

where (t) is film thickness, A absorbance. Fig.5 shows the absorption coefficient increased with an increase at 2% or 4% Cobalt dopant.

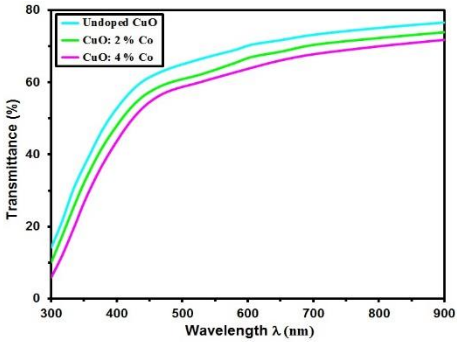

Fig. 4. Transmittance for the grown films.

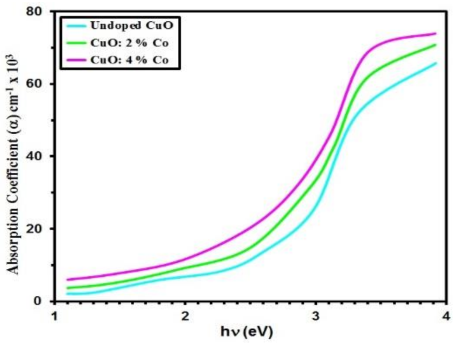

Fig. 5. α Vs hν of the grown films.

The bandgap energy E_g can be estimated by Tauc's relation [26]:

$$(\alpha h\nu) = A\left(h\nu - E_g\right)^{\frac{1}{2}} \quad (5)$$

where A is a constant, the relation between (αhν)2 and hν is plotted,

Fig. 6 shows that the Band gap of Undoped CuO sample was 2.12 eV. This decreased slightly with increasing doping concentration and became 2.08 eV for CuO: 2% Co and 2.04 eV for CuO: 4% Co, Table (1) represent the values of band gap.

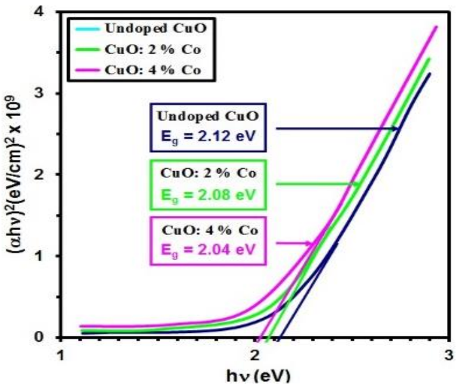

Fig. 6. (αhν)2 Vs hν of grown films.

As important optical parameters, the refractive index (n) and the extinction coefficient (k) were determined using relations 6 and 7 [27, 28].

$$n = \left(\frac{1+R}{1-R}\right) + \sqrt{\frac{4R}{(1-R)^2} - K^2} \quad (6)$$

$$k = \frac{\alpha\lambda}{4\pi} \quad (7)$$

The variation of n and k values with wavelength are shown in figures (7) and (8) respectively. There is a clear increase in n and k values with increasing Co doping ratio.

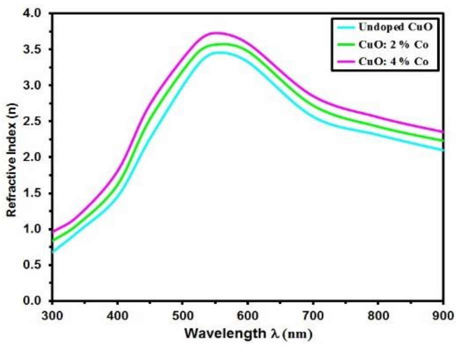

Fig. 7. Refractive Index for grown films.

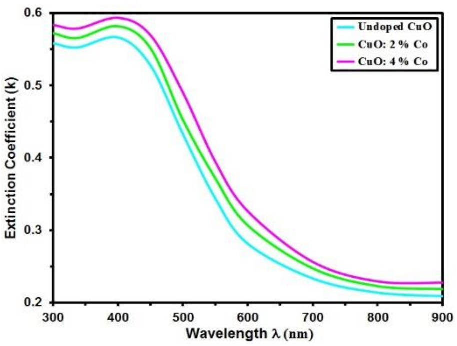

Fig. 8. Extinction coefficient (k) of the grown films.

4. Conclusions

Transparent oxide semiconductor thin films of undoped CuO and CuO: Co films have been successfully grown by SPT. XRD analysis have revealed that the peak of the max-imum intensity matches to the preferred orientation (200) for CuO films at 4% Cobalt. The Grain size is about (11.73 – 13.34) nm, whereas the strain increased from 2.98 to 2.59. AFM image showed that average particle size in the area of 41.35 nm to 32.46 nm with undoped CuO and CuO:4% Co nm respectively, transmittance decreased by the increment Cobalt doping, the absorption coefficient increased with an increase at 2% or 4% Cobalt dopant, optical bandgaps were calculated. The optical band gap decrease with increasing Cobalt dopant content from 2.12 to 2.04 eV. n and k values increased with increasing the Cobalt doping ratio.

References

[1] N. Michael, D. E. Simon, J. Thin Solid Films **516**, 1468 (2008).
[2] S. D. Davis, A. A. Harry, California Institute of Technology, 2009.
[3] M. Muhibbullah, M. O. Hakim, M. G. M. Choudhury, Thin Solid Films **423**, 103 (2003)
[4] P. Nova, Electrochim.Acta **30**, 1687 (1985)
[5] P. Novak, Electrochim. Acta **31**, 1167 (1986)
[6] L. Liao, Z. Zhang, B. Yan, Z. Zheng, Q. L. Bao, T. Wu, C. M. Li, Z. X. Shen, J. X. Zhang, H. Gong, J. C. Li, T. Yu, Nanotechnology **20**, 085203 (2009)
[7] D. Arun Kumar, Francis P. Xavier. J. Merline Shyla, Applied Science Research, 2174 (2012).
[8] Chun-Lung Chu, Hsin-Chun Lu, Chen-Yang Lo, Chi-You Lai, Yu-Hsiang Wan, Physical B Condensed Matter **404**, 4831 (2009)
[9] A. Parreta, Phys. Stat. Sol. **155**, 399 (1996).
[10] Yasukawa Kawazoe, Hyodo, Kurita, Yanagi Hosono **389**, 939 (1997).
[11] A. A. Ogwu, E. Bouquerel, O. Ademosu, S. Moh, E. Crossan, F. Placido, Acta Materialia **53**, 5151 (2005).
[12] T. A. Darma, F. Ogwu, Placido, Materials Technology: Advanced Performance Materials **26**, 28 (2011).
[13] H. Lu, C. Chu, C. Lai, Y. Wang, Thin Solid Films **517**, 4408 (2009).
[14] Papadimitropoulos, G. N. Vourdas, V. Vamvakas, D. Davazoglou, Thin Solid Films **515**, 2428 (2006).
[15] K. J. Vyas Muthe, S. Narang, D. Aswal, S. Gupta, D. Bhattacharya, R. Pinto, G. Kothiyal, S. Sabharwal, Thin Solid Films **324**, 37 (1998).
[16] Morrison, E. D. Gutiérrez-Tauste, C. Domingo, E. Vigil, J. Ayllón, Thin Solid Films **517**, 5621 (2009).
[17] P. R. Markworth, X. Liu, J. Y. Dai, W. Fan, T. J. Marks, TR. P. H. J. Chang, Mater. Res. **16**, 2408 (2001)
[18] T. D. Golden, M. G. Shumsky, U. Zhou, R. A. Vander Werf, R. A.Van Leeuwen, J. A. Switzer, Chem. Mater. **8**, 2499 (1996)
[19] S. C. Ray, Sol. Energy Mater. Sol. Cells **68**, 307, (2001)
[20] A. Chen, H. Long, X. Li, Y. Li, G. Yang, P. Lu, Vacuum **83**, 927, (2009)
[22] T. Kosugi, S. J. Kaneko, Am. Chem. Soc. **81**, 3117 (2004).
[23] L. C. Chen, Materials Science in Semiconductor Processing **16**(5), 1172(2013).
[24] X. Zhang, D. Zhang, X. Ni, H. Zheng, Solid-State Electronics **52**(2), 245 (2008).
[25] X. Gou, G. Wang, J. Yang, J. Parka, D. Wexlera, Journal of Materials Chemistry **18**(9), 965 (2008).
[26] J. Tamaki, K. Shimanoe, Y. Yamada, Y. Yamamoto, N. Miura, N. Yamazoe, Sensors and Actuators B: Chemical **49**(1), 121 (1998).
[27] S. Yatendra, A. Anshul, S. Rohit, R. Vibha, D. Sahab, Int. J. Hydrogen. Energ. **29**, 131 (2004).
[28] Armelao Lidia, Davide Barreca, Manuel Bertapelle, Gregorio Bottaro, Cinzia Sada, Eugenio Tondello, Materials Research Society **737**, 27 (2003).